On a new theoretical calibration of the Stömgren hk metallicity index: NGC 6522 as a first test case [1]

A. Calamida[2], G. Bono[3], C. E. Corsi[2], G. Iannicola[2], V. Ripepi[4], B. Anthony-Twarog[5], B. Twarog[5], M. Zoccali[6], R. Buonanno[3], S. Cassisi[7], I. Ferraro[2], F. Grundahl[8], A. Pietrinferni[7], L. Pulone[2]

ApJL, accepted on October 20, 2011

ABSTRACT

We present a new theoretical calibration of the Strömgren metallicity index hk using α-enhanced evolutionary models transformed into the observational plane by using atmosphere models with the same chemical mixture. We apply the new Metallicity–Index–Color (MIC) relations to a sample of 85 field red giants (RGs) and find that the difference between photometric estimates and spectroscopic measurements is on average smaller than 0.1 dex with a dispersion of σ= 0.19 dex. The outcome is the same if we apply the MIC relations to a sample of eight RGs in the bulge globular cluster NGC 6522, but the standard deviation ranges from 0.26 (hk, v–y) to 0.49 (hk, u–y). The difference is mainly caused by a difference in photometric accuracy. The new MIC relations based on the Ca–y

[1]Based on observations collected with the 1.54m Danish telescope (ESO, La Silla). Period 65

[2]INAF-Osservatorio Astronomico di Roma, Via Frascati 33, 00040, Monte Porzio Catone, Italy; annalisa.calamida@oa-roma.inaf.it, corsi@oa-roma.inaf.it, ferraro@oa-roma.inaf.it, giacinto@oa-roma.inaf.it, pulone@oa-roma.inaf.it

[3]Università di Roma Tor Vergata, Via della Ricerca Scientifica 1, 00133 Rome, Italy; bono@roma2.infn.it, buonanno@roma2.infn.it

[4]INAF - Osservatorio Astronomico di Capodimonte, Via Moiariello 16, 80131 Napoli; ripepi@na.astro.it

[5]Department of Physics and Astronomy, University of Kansas, 1082 Malott,1251 Wescoe Hall Dr., Lawrence, KS 66045-7582; bjat@ku.edu, btwarog@ku.edu

[6]Pontificia Universidad Católica de Chile, Departemento de Astronomia y Astrofisica, Avda. Libertador Bernardo OHiggins 340, Santiago, Chile; mzoccali@astro.puc.cl

[7]INAF-Osservatorio Astronomico di Collurania, via M. Maggini, 64100 Teramo, Italy; cassisi@oa-teramo.inaf.it, adriano@oa-teramo.inaf.it

[8]Department of Physics and Astronomy, Aarhus University, Ny Munkegade, 8000 Aarhus C, Denmark; fgj@phys.au.dk

color provide metallicities systematically more metal-rich than the spectroscopic ones. We found that the Ca-band is affected by Ca abundance and possibly by chromospheric activity.

Subject headings: stars: abundances — stars: evolution

1. Introduction

The intermediate-band Strömgren photometric system (Strömgren 1966) has, for stars with spectral types from A to G, several indisputable advantages when compared with broad-band photometric systems.

i) the Strömgren index $m_1 = (v - b) - (b - y)$ was specifically devised to estimate stellar metallicity of both evolved (horizontal branch [HB], red-giant branch [RGB]) and main sequence stars (Hilker & Richtler 2000; Anthony-Twarog & Twarog 2000; Calamida et al. 2007, hereafter CA07), while the hk index, defined as $(Ca - b) - (b - y)$ (Twarog & Anthony-Twarog 1991), replaces the v with the Ca filter centered on the $CaII$ H and K lines, and it is *primarily* sensitive to the Ca star abundance. The hk, b–y plane has been adopted to estimate the metallicity of both RG (Anthony-Twarog, Twarog, & Craig 1995) and RR Lyrae stars (Baird 1996; Rey et al. 2000). The main advantage of Strömgren metallicity indices over stellar spectroscopy is that they provide simultaneous metallicity estimates for large samples of stars. However, the use of the Strömgren indices does require precise multiband photometry and absolute calibration.

ii) The v filter is strongly affected by two CN molecular absorption bands ($\lambda = 4142$ and $\lambda = 4215$ Å). Stars with an over-abundance of carbon (C) and/or nitrogen (N), i.e. CH- and/or CN-strong stars, will have, at fixed color, larger m_1, a fundamental property for identifying stars with different CNO abundances in Globular Clusters (GCs, CA07, Calamida et al. 2009).

iii) The hk index is based on the $CaII$ H, K lines that, at fixed metal abundance, are stronger than weak metallic lines falling across the v filter. This means that the hk index in the metal-poor regime is more sensitive to metallicity changes than m_1. For cool stars, saturation of the $CaII$ lines leads to a reversal of this trend in the metal-rich regime (Anthony-Twarog, Twarog, & Craig 1995).

iv) Lee et al. (2009b), using u, v, b, y, Ca data for 37 GGCs, found that most of them show a discrete or broad RGB in the y, hk plane, and suggested a spread in Ca and/or heavy element abundance in these GGCs.

2. Observations and calibration of the hk metallicity index.

Ca-uvby Strömgren images were collected during two observing nights (July 6-7, 2000) with the 1.54m Danish Telescope (ESO) and the DFOSC camera, with a pixel scale of 0.39″and a field of view of 13.7′×13.7′. The pointing was centered on the Baade's Window (α = 18:03:34, δ = -30:04:10), including NGC 6522. We secured 16 images ($4y, 4b, 2v, 2Ca, 2u$), with exposure times ranging from 60s (y) to 1000s (Ca), and seeing between ∼1.″2 and ∼1.″6. Standard stars were selected from the catalog by Hauck & Mermilliod (1998) and observed across each night.

The photometry was performed with DAOPHOT IV/ALLFRAME (Stetson 1987, 1994) and aperture photometry on the standards with ROMAFOT (Buonanno & Iannicola 1989). Extinction coefficients were estimated from observations of standards at different air-mass values. Calibration curves from the two observing nights agreed quite well and we selected the best photometric night, July 6, as the reference night. The final calibrated catalog includes ≈80,000 stars with an accuracy of $\sigma_y \lesssim 0.1$ and $\sigma_{v-y} \lesssim 0.2$ mag at $y \approx 20$ mag. The accuracy of the calibration is ~ 0.02 mag for the y, b, v bands and ~ 0.05 mag for the Ca, u bands.

In this investigation we are focusing on NGC 6522, therefore the final catalog was restricted by photometric accuracy and star position. Only stars with distances from the cluster center (α = 18:03:34, δ = -30:02:02) in the range 0.65′– 1.65′ were plotted in the y, v–y (left panel), y, u–y (middle) and y, Ca–y (right) Color-Magnitude Diagrams (CMDs) of Fig. 1. The cluster center was excluded due to crowding, but stars up to about 1.5 the half-light radius (r_h = 1.0′, Harris 2003) are selected. The entire photometric catalog will be presented in a forthcoming paper.

In order to validate current absolute calibration we compared cluster photometry with both theoretical predictions and Strömgren photometry of NGC 288 (CA07). We adopted this GC, because current spectroscopic measurements indicate an iron abundance ([Fe/H]= -1.32±0.02 dex) similar to NGC 6522 ([Fe/H]= -1.45±0.08 dex, Carretta et al. 2009).

We adopted a true distance modulus for NGC 6522 of $\mu_0 = 13.91$ and a mean reddening $E(B-V) = 0.55$ (Barbuy et al. 1998). The extinction coefficients for the Strömgren colors were estimated by applying the Cardelli et al. (1989) reddening relation and $R_V = A_V/E(B-V) = 3.13$, according to the reddening dependence of R_V on $E(B-V)$ (Olson 1975, see also Barbuy et al. 1998) We found: $E(b-y) = 0.69 \times E(B-V)$, $E(v-y) = 1.31 \times E(B-V)$, $E(u-y) = 1.82 \times E(B-V)$ and $E(Ca-y) = 1.46 \times E(B-V)$.

The blue and the red solid lines in Fig. 1 show two cluster isochrones at fixed age (t = 13 Gyr) and different chemical compositions, namely $Z = 0.002, Y = 0.248$ and $Z = 0.004, Y =$

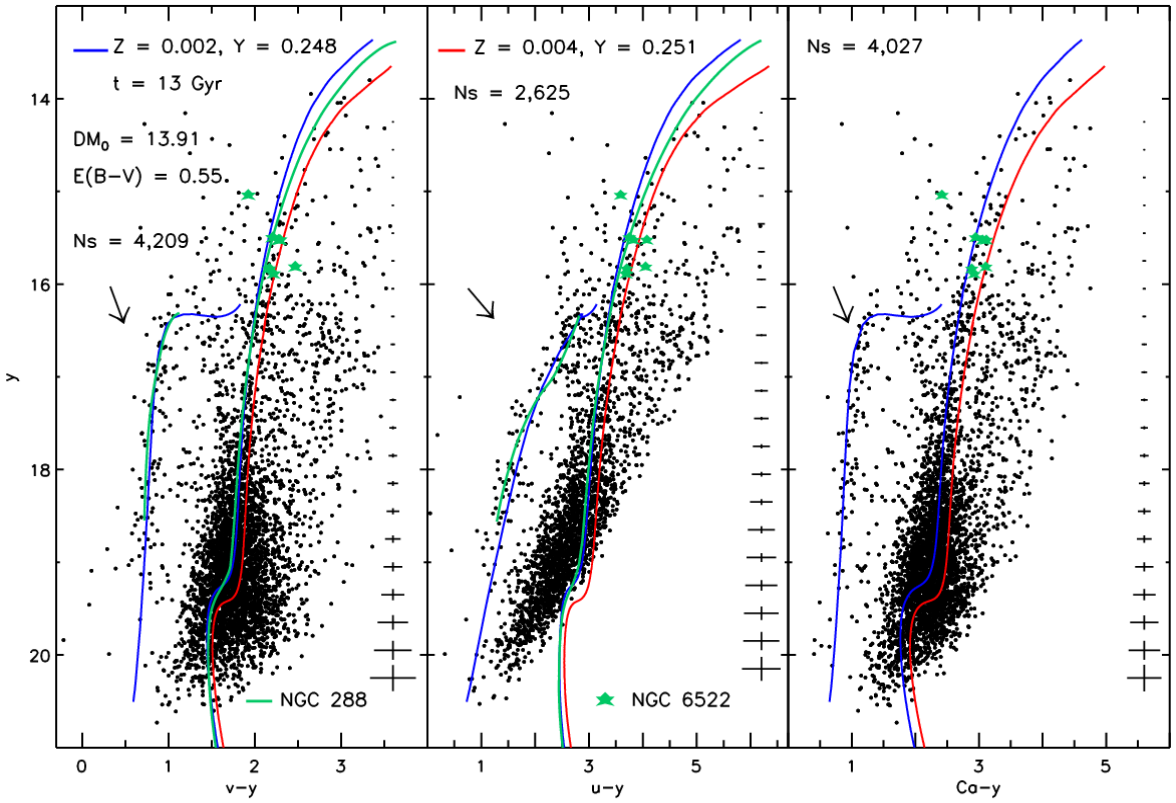

Fig. 1.— y, v–y, u–y, Ca–y CMDs of NGC 6522. Stars were selected according to distances from the center ($0.65' \leq r \leq 1.65'$) and photometric accuracy. Error bars display intrinsic errors in color and in magnitude, while the arrows show the reddening directions. The red and the blue solid lines display two cluster isochrones at fixed age and for different chemical compositions and the predicted ZAHB for $Z = 0.002$. The green solid lines show the ridge lines of NGC 288. The adopted true distance modulus and cluster reddening are labeled. The green stars mark the eight cluster RGs observed spectroscopically by Barbuy et al. (2009).

0.251, and the predicted Zero Age Horizontal Branch (ZAHB) for $Z = 0.002$. Isochrones are from the BASTI data base and are based on α-enhanced ($[\alpha/Fe] = 0.4$) evolutionary models (Pietrinferni et al. 2006, hereafter PI06), transformed into the observational plane using atmosphere models computed assuming α-enhanced mixtures. Data plotted in Fig. 1 show that theory and observations, within the errors, agree quite well over the entire magnitude range.

In particular, the two isochrones bracket the RGs with known metal abundance, i.e.

$-0.96 \lesssim$ [M/H] $\lesssim -0.66$ dex ($-1.31 \lesssim$ [Fe/H] $\lesssim -1.01$ dex). The small discrepancy between the ZAHB and the HB might be due to the effect of differential reddening, which also produces part of the RGB spread. The reddening vector is shown for each CMD in Fig. 1.

The green solid lines show the ridge lines of NGC 288 along the RGB and the HB. To compare the two GCs we adopted a true distance modulus of $\mu_0 = 14.67$ (Ferraro et al. 1999) and a reddening of $E(B-V) = 0.01$ (CA07). Unfortunately, Ca-band photometry for this cluster is not available.

The RGB ridge line of NGC 288 is systematically bluer than RGs in NGC 6522, thus suggesting that the latter GC is slightly more metal-rich than the former one. This result agrees quite well with recent iron abundances for eight RGs (green stars) provided by Barbuy et al. (2009, hereafter BA09). The measurements are based on high-resolution spectra collected with FLAMES/GIRAFFE at the VLT (ESO) and give [Fe/H]= -1.0±0.2 dex on the Carretta & Gratton (1997) metallicity scale.

The consistency between theoretical and empirical scenario is further supported by the evidence that the NGC 288 ridge lines agree quite well with more metal-poor ($Z = 0.002$) evolutionary predictions.

Independent Metallicity–Index–Color (MIC) relations are derived using cluster isochrones based on α-enhanced evolutionary models (PI06). Theoretical predictions were transformed into the observational plane by adopting bolometric corrections (BCs) and Color–Temperature Relations (CTRs) based on atmosphere models computed assuming the same heavy element abundances (PI06, Castelli & Kurucz 2006). The Vega flux adopted is from Castelli & Kurucz (1994)[1]. The metallicities adopted for the calibration are: Z=0.0001, 0.0003, 0.0006, 0.001, 0.002, 0.004, and 0.01. We neglected more metal-rich structures because the hk index loses sensitivity in the metal-rich regime (Anthony-Twarog & Twarog 1998, hereafter ATT98, and references therein). The adopted Z values indicate the global abundance of heavy elements in the chemical mixture, with a solar metal abundance of $(Z/X)_\odot = 0.0245$.

To unredden the hk index we adopted $E(hk) = -0.155 \times E(b–y)$ (Anthony-Twarog et al. 1991, hereafter AT91). Together with the unreddened index, hk_0, we also derive independent MIC relations for the reddening-free parameter $[hk] = hk_0 + 0.155 \times (b–y)$, to overcome deceptive uncertainties caused by differential reddening.

Fig. 2 shows the seven isochrones plotted in the $[hk]$, $v–y$ plane, covering the evolu-

[1]The complete set of BCs, CTRs and the Vega flux are available at http://wwwuser.oat.ts.astro.it/castelli

tionary phases from the base of the RGB to the tip. Note the nonlinearity of the hk, v–y relations for RGs and the decrease in sensitivity of the hk index when moving from the metal-poor to the metal-rich regime ([M/H] $\sim$ -0.5 dex), as originally suggested by ATT98.

To select the hk_0 and $[hk]$ values along the individual isochrones we follow the same approach adopted for the calibration of the m_1 index (CA07). A multilinear regression fit was performed to estimate the coefficients of the MIC relations for the hk_0 and the $[hk]$ indices as a function of four Color Indices (CIs): b–y, v–y, Ca–y, u–y:

$$\begin{aligned} hk_0 = \alpha + \beta\,[\mathrm{M/H}] + \gamma\,CI_0 + \delta\,(CI_0 \times hk_0) + \epsilon\,CI_0^2 + \\ \zeta\,hk_0^2 + \eta\,(CI_0^2 \times hk_0) + \theta\,(CI_0 \times hk_0^2) + \iota\,(CI_0^2 \times hk_0^2) + \\ \kappa\,(CI_0 \times [\mathrm{M/H}]) + \lambda\,(hk_0 \times [\mathrm{M/H}]) \end{aligned}$$

where the symbols have their usual meaning. The adoption of eleven terms, compared to the four of the m_1 calibration, is due to the nonlinearity of the hk_0 vs CI_0 relations for RGs. The coefficients of the fits, together with their uncertainties, for the eight MIC relations, are listed in Table 1.

3. Validation of the new calibration of the hk index

In order to validate the new calibration of the hk index we estimate the metallicity of field RGs for which Anthony-Twarog & Twarog (1994, hereafter ATT94) and ATT98 collected both *Ca-uvby* photometry and high-resolution spectra. We end up with a sample of 96 RGs. For 28 of them we retrieve from the VO database the Ca and Mg abundances of Fulbright (2000, hereafter FU00), from which a proxy of the α-enhancement is estimated either as $[\alpha/Fe] = [Ca/Fe]$ or as $[\alpha/Fe] = [(Ca{+}Mg)/Fe]$. The metallicity range covered by our MIC relations is $-2.6 <$ [Fe/H] < -0.6 dex, but we select stars with $-2.7 <$ [Fe/H] < -0.5 dex to account for uncertainties in spectroscopic abundances and in the metallicity scale (Kraft & Ivans 2003). We end up with 85 RGs of which 24 have Ca,Mg abundance measurements.

We plot the difference between photometric and spectroscopic metallicities for the 85 field RGs as a function of their spectroscopic metal abundances in Fig. 3. Photometric abundances are estimated via the hk_0, v–y (panels a,c) and the hk_0, Ca–y relations (b,d). The global metallicity [M/H] is estimated adopting the Salaris et al. (1993) formula and either the $[Ca/Fe]$ (panels a,b) or the $[(Ca + Mg)/Fe]$ measurement (c,d) for the 24 RGs in common with FU00 (red dots), or a constant α-enhancement for the remaining stars of

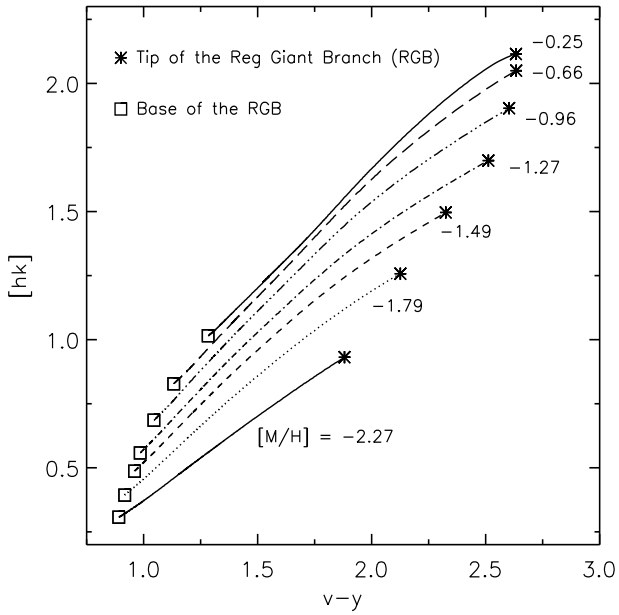

Fig. 2.— $[hk]$ (v–y) plane for isochrones at fixed cluster age (t=13 Gyr) and different chemical compositions ([M/H], see labeled values). The evolutionary phases range from the base of the RGB (squares) to the tip (asterisks). Evolutionary tracks were computed by assuming $\alpha-$enhanced chemical mixtures (PI06) and transformed by adopting atmosphere models with the same $\alpha-$enhancement.

$[\alpha/Fe]$=0.4 dex (RGs with [Fe/H] $\lesssim$ -0.8 dex) and $[\alpha/Fe]$=0.15 dex (RGs with [Fe/H] $>$ -0.8 dex, black). Data plotted in Fig. 3 show that the difference between spectroscopic measurements and photometric estimates is, on average, of the order of 0.1 dex when using the hk_0, v–y relation ($\sim$ -0.07$\pm$0.02 dex, $[\alpha/Fe] = [Ca/Fe]$; $\sim$ -0.09$\pm$0.02 dex, $[\alpha/Fe] = [(Ca + Mg)/Fe]$), or the hk_0, Ca–y relation ($\sim$ -0.09$\pm$0.02 dex; $\sim$ -0.11$\pm$0.02 dex). To overcome subtle uncertainties in the estimate of the mean difference we adopt the Biweight algorithm (Fabrizio et al. 2011). The intrinsic dispersion of the different MIC relations is smaller than 0.2 dex and caused either by photometric errors, or by reddening uncertainties, or by spectroscopic errors. The error bars in the bottom panel of Fig. 3 display the mean error for the spectroscopic measurements ($\sigma([\mathrm{M/H}]_{\mathrm{spec}}) \sim 0.15$ dex), estimated as the average of both the internal dispersion about the mean of [Fe/H] measurements, the uncertainty due to the transformations into the standard metallicity scale (see column 8 in Table 2 and column 7 in Table 4 of ATT98), and the internal uncertainties of the $[Ca/Fe]$ and $[Mg/Fe]$ measurements by FU00. The CH-strong stars (HD 55496, HD 135148, BD-01 2582, BD+04 2466, CD-62 1346, diamonds) do not show, in contrast with the metallicity based

on the m_1 MIC relations (see CA07), any peculiar discrepancy between photometric and spectroscopic metallicities. On the other hand, star HD 84903 (asterisk), which might be affected by weak chromospheric emission in the core of the $CaII$ K line (ATT98), showed a large discrepancy (Δ[M/H] $\approx$ -0.4 dex) when using the m_1 MIC relations. We now adopt for HD 84903 [Fe/H]= -2.6 dex, estimated accounting non-LTE effects by Thévenin et al. (1999). The difference between photometric and spectroscopic abundances is now inside current uncertainties (Δ[M/H] $\approx$ -0.2 dex). The star HD 44007 (cross) was already discussed in ATT98, since the reddening correction is still uncertain. Photometric metallicities for two metal-rich stars (HD 35179, HD 7595) with [M/H] $>$ -0.60 dex, are systematically more metal-poor by $\sim$ 0.5 dex than spectroscopic measurements. Such a discrepancy might be due either to reddening uncertainties, or to the reduced sensitivity of the hk index in the metal-rich regime.

We were not able to validate current calibrations with the spectroscopic abundances of RGs in Baade's Window field (Zoccali et al. 2008), since almost all of them are more metal-rich than [Fe/H]= -0.5 dex, therefore outside the metallicity range covered by the new MIC relations.

To further validate current calibrations, we apply the MIC relations to estimate the metallicity distribution of RGs in NGC 6522. The catalog is selected in star position as described in §1, in magnitude ($y < 18.0$ mag), in photometric accuracy ($\sigma(v,b,y) < 0.03$ and $\sigma(Ca) < 0.02$ mag), and in surface gravity ($[c] = c_1 - 0.2 \times (b-y) < 0.35$ mag), ending up with 51 RGs. We downloaded the catalog of proper motions across the Galactic bar by Sumi et al. (2003) from the VO database, for a region of $15' \times 15'$ across the cluster center. The match with our catalog gives $\sim 13,200$ stars in common. The accuracy of the proper motions is $\sim$ 1 mas/yr, while the accuracy of the positional match is $\lesssim 1''$. We further select our sample with $-2 < pm(\alpha) < 6$ and $-2 < pm(\delta) < 2$ mas/yr, following the classification made by Sumi et al. of RG, red-clump and disc stars (see their Fig. 8). Since the proper motions of field stars partly overlap with those of cluster stars, we cannot exclude contamination in the final sample of 28 candidate cluster RGs.

Fig. 4 shows the difference between photometric metallicities of the 28 candidate RGs estimated adopting the hk_0, v–y MIC relation and the relations based on hk_0 and the b–y, Ca–y, u–y colors plotted versus metallicities estimated with hk_0, v–y.

By using the eight RGs (red dots) in common with the spectroscopic sample (BA09), we find that the difference (Biweigth mean) between photometric and spectroscopic metallicity[2]

[2]The α-element abundance of the spectroscopic RGs is estimated as $[\alpha/Fe] = [(Ca+Si+Mg)/Fe]$, while their [Fe/H] is transformed in the Zinn & West (1984) scale using the Carretta & Gratton (1997) relation.

is minimal not only for the hk_0, v–y ($< \Delta([\mathrm{M/H}]_{\mathrm{phot}} - [\mathrm{M/H}]_{\mathrm{spec}}) > \simeq -0.02 \pm 0.01$, σ=0.26 dex), but also for the hk_0, b–y ($\simeq -0.05 \pm 0.01$, σ=0.38 dex) and the hk_0, u–y ($\simeq -0.03 \pm 0.01$, σ=0.49 dex) MIC relation. The difference becomes larger when using the hk_0, Ca–y ($\simeq 0.22 \pm 0.01$, σ=0.45 dex) relation. The difference is marginally larger when using the MIC relations based on the reddening free index. In particular, it is $\simeq -0.12 \pm 0.01$, σ=0.67 for the $[hk]$, Ca–y and $\simeq -0.17 \pm 0.01$, σ=0.43 for the $[hk]$, u–y relations. The difference between unreddened and reddening free MIC relations is mainly due to the sum in quadrature of the intrinsic photometric error. The evidence that the MIC relations using the Ca-band both in the metallicity index and in the color index show either the largest difference or the largest dispersion suggest that the discrepancy might be intrinsic. Data plotted in Fig. 4 further support this finding. Indeed, metallicity estimates based on the hk_0, b–y and on the hk_0, u–y relations agree reasonably well with those based on the hk_0, v–y relation ($< \Delta([\mathrm{M/H}]_{\mathrm{by,\ uy}} - [\mathrm{M/H}]_{\mathrm{vy}}) > \simeq 0.0 \pm 0.02$ and $\simeq -0.01 \pm 0.02$ with $\sigma = 0.26$ and 0.19 dex, respectively.) On the other hand, the metallicity estimates based on the hk_0, Ca–y relation are on average $\approx$0.3 dex more metal-rich than those based on the hk_0, v–y relation. The difference might be due to the fact that the hk_0, Ca–y relation is more sensitive to the Ca abundance than the other relations. Moreover, Anthony-Twarog, Twarog, & Craig (1995) suggested that the hk index of RGs in M22 might be affected by a continuous absorption in the wavelength range between $3,900$ and $4,100$ Å (see also Bond & Neff 1969). We plan to provide a more quantitative analysis of this effect in a forthcoming paper. Another possible culprit might be the chromospheric activity, since this phenomenon causes an emission in the core of the $CaII\ K$ line (Smith, Dupree, & Churchill 1992; Dupree et al. 1999; Lee et al. 2009a). Unfortunately, the high-resolution spectra collected by BA09 do not cover the wavelength region of $CaII\ H\ K$ lines.

The photometric metallicity distributions show a well-defined main peak around [M/H] ~ -0.95 dex and two shoulders at [M/H] $\sim$ -1.4 and -0.5 dex. These features agree quite well with the spectroscopic metallicity distribution, which shows two peaks at [M/H] ~ -1.1 and [M/H] ~ -0.85 dex, with the latter one including $\sim 10\%$ of the stars. The difference between the main and the secondary peak might be due to an enhancement either in Ca or in other heavy elements. We cannot reach a firm conclusion concerning the few more metal-poor ([M/H] $\lesssim$ -1.4 dex) outliers, since the standard deviations of the MIC relations range from $\sim$ 0.25 to 0.5 dex. They might be either field bulge stars or objects affected by differential reddening.

Lee et al. (2009a,b) found a double peaked distribution when applying their hk_0, b–y metallicity relation to stars in NGC 1851. This is a peculiar GGC, with a split along the sub-giant and the RG branches, that might be due to the presence of two stellar populations with different CNO abundance (CA07; Cassisi et al. 2008). The secondary peak in the

metallicity distribution includes $\sim 18\%$ of the RGs (Lee et al. 2009a), including three Ca-enhanced stars (Yong & Grundahl 2008) and three CN-strong stars (Hesser et al. 1982) with enhanced abundances of Ba and Sr.

The above results indicate that possible differences in cluster RG colors including the Ca-band should be cautiously treated, since they might be caused either by changes in Ca and/or by other heavy elements or by molecular bands.

We show that the Strömgren hk index is a good diagnostic to estimate the global metal abundance of field and cluster RGs, and it can be also adopted to detect stars affected by Ca enhancement. Moreover, the hk index is more sensitive than the m_1 index in the metal-poor regime, and is less affected by CN, CH peculiarities. The current MIC relations have been validated by adopting RGs in NGC 6522 and field RGs with known spectroscopic abundances, and provide metallicities with an accuracy better than 0.2 dex. The application of the new MIC relations appear very promising not only for RGs in halo GGCs, but also to pin point metal-poor stars in the Galactic halo.

It is a real pleasure to thank F. Castelli for sending us bolometric corrections and color indices for Strömgren bands. MZ is partly supported by Proyecto FONDECYT Regular 1110393, the FONDAP Center for Astrophysics 1510003, the BASAL CATA PFB-06, the Milky Way Millennium Nucleus from ICM grant P07-021-F, and by Proyecto Conicyt Anillo ACT-86.

REFERENCES

Anthony-Twarog, B. J., Laird, J. B., Payne, D., & Twarog, B. A. 1991, AJ, 101, 1902 (AT91)

Anthony-Twarog, B. J., & Twarog, B. A. 1994, AJ, 107, 1577 (ATT94)

Anthony-Twarog, B.J., Twarog, B.A., & Craig, J. 1995, PASP, 107, 32

Anthony-Twarog, B. J., & Twarog, B. A. 1998, AJ, 116, 1922 (ATT98)

Anthony-Twarog, B. J., & Twarog, B. A. 2000, AJ, 120, 3111

Baird, S., 1996, AJ, 112, 5

Barbuy,B., Bica, E., Ortolani, S. 1998, A&A, 333, 117

Barbuy,B., et al. 2009, A&A, 507, 405 (BA09)

Bond, H. E., Neff, J. S. 1969, ApJ, 158, 1235

Buonanno, R., Iannicola, G. 1989, PASP, 101, 294

Calamida, A., et al. 2007, ApJ, 670, 400 (CA07)

Calamida, A., et al. 2009, ApJ, 706, 1277

Cardelli, J. A., Clayton, G. C., & Mathis, J. S. 1989, ApJ, 345, 245

Carretta, E., Bragaglia, A., Gratton, R., D'Orazi, V., Lucatello, S. 2009, A&A, 508, 695

Dupree, A. K., Whitney, B. A., Pasquini, L. 1999, ApJ, 520, 751

Carretta, E., Gratton, R. 1997, A&A, 121, 95

Cassisi, S., Salaris, M., Pietrinferni, A., Piotto, G., Milone, A. P., Bedin, L. R., Anderson, J. 2008, ApJ, 672, L115

Castelli, F., & Kurucz, R. L. 1994, A&A, 281, 817

Castelli, F., & Kurucz, R. L. 2006, A&A, 454, 333

Fabrizio, M., et al. 2011, PASP, 123, 384

Ferraro, F. R., Messineo, M., Fusi Pecci, F., de Palo, M. A., Straniero, O., Chieffi, A., Limongi, M. 1999, AJ, 118, 1738

Fulbright, J.P. 2000, AJ, 120, 1841 (FU00)

Harris, W.E. 2003, Catalog of Parameters for Milky Way Globular Clusters: The Database Hamilton: McMaster Univ., http://physun.physics.mcmaster.ca/∼harris/mwgc.dat

Hauck, B., & Mermilliod, M. 1998, A&AS, 129, 431

Hesser, J. Bell, R. A., Harris, G. L. H., Cannon, R. D. 1982, AJ, 87, 1470

Hilker, M., & Richtler, T. 2000, A&A, 362, 895

Kraft, R.P., Ivans, I. I. 2003, PASP, 115, 143

Lee, J.-W., et al. 2009, ApJ, 695, L78

Lee, J.-W., Kang, Y.-W., Lee, J., Lee, Y.-W. 2009, Natur., 462, 480

Olson, B.I. 1975, PASP, 87, 349

Pietrinferni, A., Cassisi, S., Salaris, M., Castelli, F. 2006, ApJ, 642, 697 (PI06)

Rey, S.-C., Lee, Y.-W., Joo, J.-M., Walker, A., Baird, S. 2000, AJ, 119, 1824

Salaris, M., Chieffi, A., & Straniero, O. 1993, ApJ, 414, 580

Smith, G.H., Dupree, A. K., & Churchill, C. W. 1992, AJ, 104, 2005

Stetson, P. B. 1987, PASP, 99, 191

Stetson, P. B. 1994, PASP, 106, 250

Strömgren, B. 1966, Ann.Rev. A&A, 4, 433

Sumi, T., Eyer, L., Wozaniak, P. R. 2003, MNRAS, 340, 1346

Thevénin, F., Idiart, T. P. 1999, ApJ, 521, 753

Twarog, B.A., Anthony-Twarog, B.J. 1991, AJ, 101, 237

Yong, D., Grundahl, F. 2008, ApJ, 672, L29

Zoccali, M., et al. 2008, A&A, 486, 177

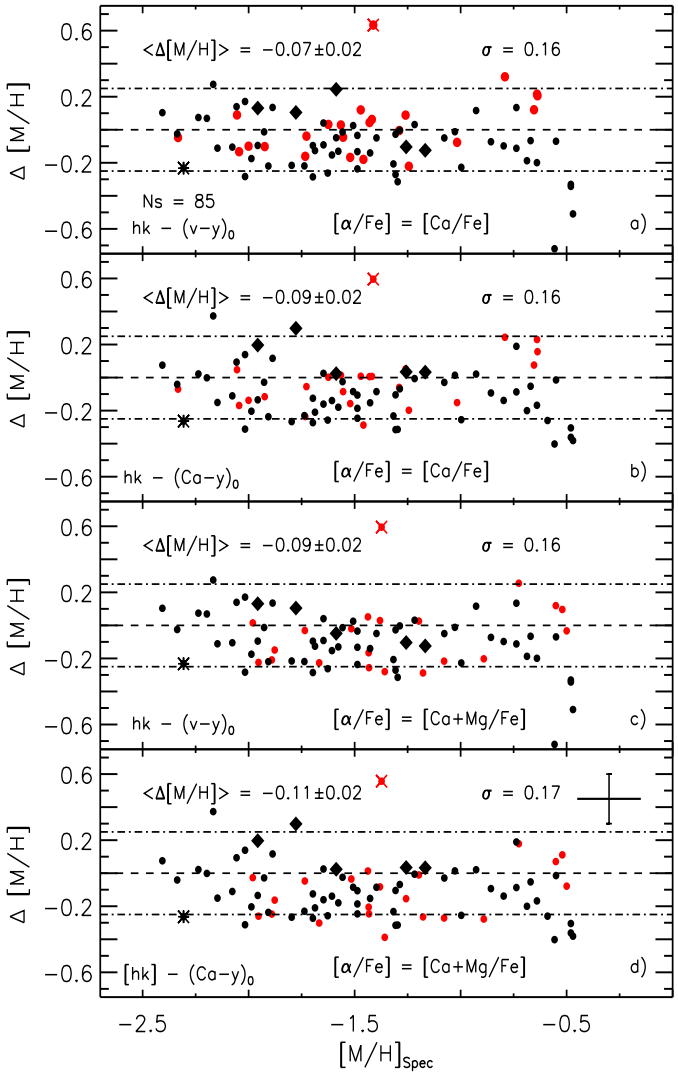

Fig. 3.— Difference between photometric and spectroscopic metallicities, Δ[M/H] = ([M/H]$_{\rm phot}$ − [M/H]$_{\rm spec}$), plotted versus [M/H]$_{\rm spec}$ for 85 field RGs by ATT94 and ATT98. Panels a) and c) display photometric metallicities based on the hk_0, v–y relation, while panels b) and d) on the hk_0, Ca–y relation. For 24 RGs the α-enhancement is estimated using either Ca (panels a),b)) or Ca and Mg measurements (panels c),d)), while for the other objects a constant α-enhancement is assumed (see text for more details). The diamonds mark the CH-strong stars, the asterisk star HD 84903, while the cross the star with an uncertain reddening (HD 44007). The error bars in the bottom panel display the mean error for the spectroscopic measurements.

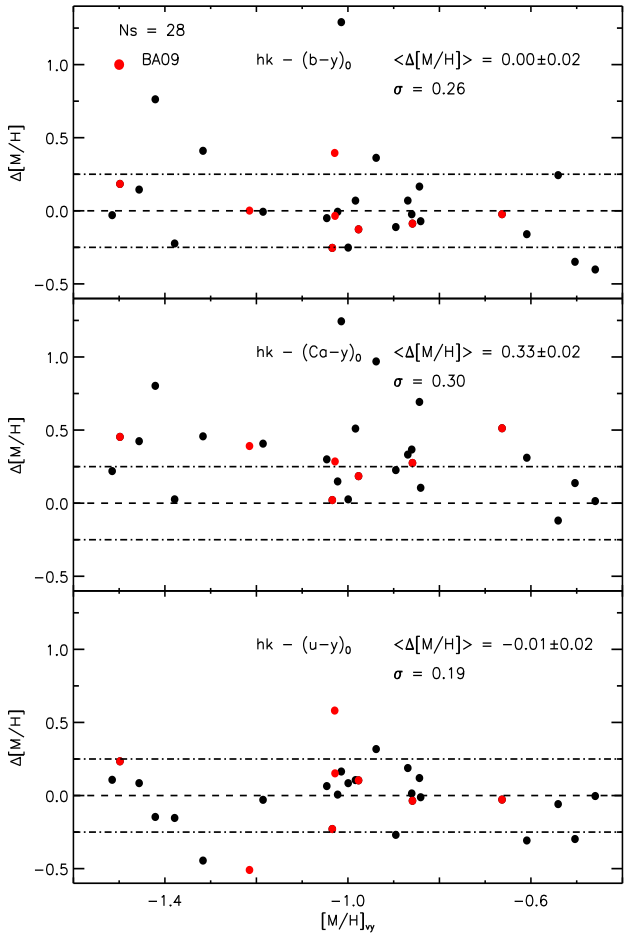

Fig. 4.— Difference between photometric metallicities estimated adopting different MIC relations, hk, b–y(top),hk, Ca–y(middle) and hk, , u–y (bottom) plotted versus the metallicity estimated with the hk, v–y relation for 28 candidate cluster RGs. The eight RGs with spectroscopic measurements are marked in red.

Table 1. Multilinear regression coefficients for the Strömgren metallicity index: $hk_0 = \alpha + \beta\,[\mathrm{Fe/H}] + \gamma\,CI_0 + \delta\,(CI_0 \times hk_0) + \epsilon\,CI_0^2 + \zeta\,hk_0^2 + \eta\,(CI_0^2 \times hk_0) + \theta\,(CI_0 \times hk_0^2) + \iota\,(CI_0^2 \times hk_0^2) + \kappa\,(CI_0 \times [\mathrm{Fe/H}]) + \lambda\,(hk_0 \times [\mathrm{Fe/H}])$.

Relation (1)	α (2)	β (3)	γ (4)	δ (5)	ϵ (6)	ζ (7)	η (8)	θ (9)	ι (10)	κ (11)	λ (12)
$hk_0, (b–y)_0$	0.125	0.116	0.756	0.860	-0.556	0.684	-0.282	-1.057	0.495	-0.019	-0.081
Error	0.010	0.009	0.172	0.297	0.142	0.047	0.144	0.045	0.032	0.027	0.012
$hk_0, (v–y)_0$	-0.009	0.096	0.615	-0.072	-0.107	0.735	0.040	-0.299	0.041	0.047	-0.133
Error	0.010	0.007	0.056	0.091	0.026	0.056	0.021	0.014	0.004	0.013	0.015
$hk_0, (Ca–y)_0$	-0.028	0.051	0.425	-0.094	-0.034	0.720	0.018	-0.176	0.016	0.050	-0.131
Error	0.010	0.010	0.035	0.140	0.032	0.155	0.010	0.018	0.002	0.017	0.029
$hk_0, (u–y)_0$	0.131	0.097	0.183	0.125	-0.018	0.616	-0.011	-0.171	0.017	0.012	-0.099
Error	0.010	0.008	0.031	0.054	0.008	0.062	0.007	0.008	0.001	0.008	0.016
$[hk], (b–y)_0$	0.162	0.105	0.657	1.030	-0.375	0.547	-0.493	-0.864	0.433	0.011	-0.070
Error	0.010	0.009	0.181	0.191	0.152	0.039	0.133	0.035	0.029	0.027	0.011
$[hk], (v–y)_0$	0.022	0.086	0.597	-0.057	-0.060	0.644	0.005	-0.247	0.039	0.064	-0.132
Error	0.010	0.006	0.058	0.091	0.031	0.051	0.019	0.012	0.004	0.013	0.014
$[hk], (Ca–y)_0$	-0.021	0.049	0.462	-0.147	-0.030	0.703	0.023	-0.157	0.013	0.053	-0.126
Error	0.010	0.010	0.038	0.172	0.043	0.174	0.011	0.017	0.002	0.019	0.031
$[hk], (u–y)_0$	0.127	0.083	0.206	0.090	-0.009	0.580	-0.013	-0.149	0.015	0.025	-0.106
Error	0.010	0.008	0.029	0.056	0.009	0.059	0.005	0.007	0.001	0.009	0.017